Afyon Kocatepe Üniversitesi Fen ve Mühendislik Bilimleri Dergisi

Afyon Kocatepe University Journal of Science and Engineering

AKÜ FEMÜBİD **23** (2023) 031205 (618-627) AKU J. Sci. Eng. **23** (2023) 031205 (618-627)

DOI: 10.35414/akufemubid.1207578

Araştırma Makalesi / Research Article

Investigation Into The Molecular Stability, Synthesis Mechanism, and Formation of Some Norcantharimide Derivatives Using AcCl or Ac_2O: A Mechanism-Based Study

Aytekin KÖSE[1]

[1]*Department of Chemistry, Faculty of Science and Letters, Aksaray University, Aksaray, Turkey*

Corresponding author e-mail: aytekinkose@aksaray.edu.tr ORCID ID: http://orcid.org/0000-0003-2448-3716*

Geliş Tarihi: 20.11.2022 Kabul Tarihi: 16.06.2023

Keywords
Chlorinated products; Norcantharimide; Amines; S_N2' mechanism

Abstract

The aim in this study was first to explain, in detail the conversion of diacetates over time into chlorinated monoacetates following ether cleavage with AcCl of norcantharimide derivatives with the help of the NMR technique and second, to verify this conversion theoretically and computationally. Ether cleavage reactions of *N*-methyl, *N*-benzyl, and *N*-acetoxyethyl-substituted norcantharimide derivatives were performed with Ac_2O or AcCl in the presence of H_2SO_4, and the mechanisms of these reactions were elucidated in detail. According to the ^1H NMR analyses of aliquots from the reactions with AcCl, *trans*-1,4-diacetates formed firstly. Upon the continuation of the reaction, *trans*-1,4-diacetates transformed into *trans*-1,2-chloroacetates via an S_N2' mechanism. Additionally, this explanation was further supported by the soft theoretical and physical calculations.

AcCl veya Ac_2O Kullanılarak Bazı Norkantarimid Türevlerinin Moleküler Kararlılık, Sentez Mekanizması ve Oluşumunlarının İncelenmesi: Mekanizma Tabanlı Bir Çalışma

Anahtar Kelimeler
Klorlanmış ürünler; Norkantarimid; Aminler; S_N2' mekanizması

Öz

Bu çalışmadaki amaç, ilk olarak norkantarimid türevlerinin AcCl ile eter parçalanmasından sonra oluşan diasetatların zamanla klorlu monoasetatlara dönüşümünü NMR tekniği yardımıyla detaylı olarak açıklamak ve ikinci olarak bu dönüşümü teorik ve hesaplamalı olarak doğrulamaktır. *N*-metil, *N*-benzil ve *N*-asetoksietil sübstitüe norkantarimid türevlerinin eter parçalanma reaksiyonları Ac_2O veya AcCl ile H_2SO_4 varlığında gerçekleştirildi ve bu reaksiyonların mekanizmaları detaylı olarak açıklandı. AcCl ile yapılan reaksiyonlardan alınan örneklerin ^1H NMR analizlerine göre, önce *trans*-1,4-diasetatlar oluştu. Reaksiyonun devam etmesi ile *trans*-1,4-diasetatlar, S_N2' mekanizması yoluyla *trans*-1,2-kloroasetatlara dönüştü. İlave olarak, bu açıklama teorik ve fiziksel hesaplamalarla daha da desteklendi.

1. Introduction

Cantharidin is a natural compound, and its use as a potential anticancer agent dates back to 1264 (Nickolls and Teare 1954, Wang 1989, Lin *et al*. 1998). This molecule belongs to the terpenoid class, which is used for curative purposes in numerous treatments in traditional Chinese medicine (Wang 1989). Cantharidin and its structural derivatives norcantharidin (**1**) and, norcantharimide (**2**) and their analogs **3** and **4** (Figure 1) attract biomedical interest due to their small size, easy modifiability, and ability to pass through cell membranes without requiring energy. Although cantharidin is suitable for use for chemotherapeutic purposes, it has limited usage due to its known toxic effects (Tagwireyi *et al*. 2000). Therefore, there is a need for new cantharidin derivatives with increased

therapeutic effect and reduced toxicity. For this purpose, scientists have long focused on the synthesis of these new derivatives and on studies to improve the products' therapeutic index.

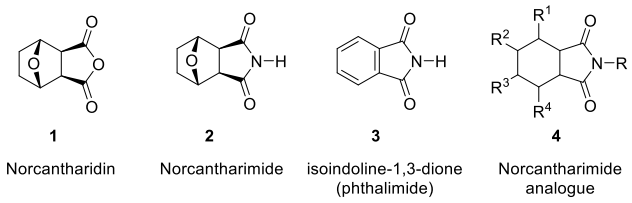

Figure 1. Molecular structures of norcantharidin (**1**), norcantharimide (**2**), isoindoline-1,3-dione (**3**), and norcantharimide analog **4**.

Norcantharidin (**1**), norcantharimide (**2**), isoindoline-1,3-dione (**3**) and its analogs **4** are preferred due to their small molecular structures, ability to be synthesized by short-step syntheses, using cheap and simple chemical methods, and the above mentioned biochemical properties. It is possible to synthesize norcantharimides from cantharidin and norcantharidin, which are structurally anhydrides, using primary aromatic/aliphatic amines and thus the synthesis of norcantharimide derivatives having potentially different bioactivity becomes possible. Recently, Kara and co-workers synthesized norcantharimide analogs containing different functional groups on the cyclohexane ring starting from 3-sulfolene. They also investigated the synthetic routes for norcantharimide derivatives and their photophysical properties (Tan *et al*. 2011 and 2014). In this study, the ether cleavage reaction mechanism of norcantharimide derivatives using Ac_2O and AcCl was examined in detail. The compounds used were synthesized and characterized by the NMR technique previously (Köse *et al*. 2017 and 2020). Here, detailed NMR spectroscopy studies depending on the specified reaction time intervals, conversions between of *trans*-1,4-diacetates and *trans*-1,2-chloroacetates, and detailed and descriptive synthesis mechanisms of the products were discussed and explained, unlike in the previous work (Köse *et al*. 2020). Moreover, the products that formed at specified time intervals were identified and the data from these conversions were graphed. All reactions are solvolysis reactions. In contrast to our previous work, in this study, soft density functional theory (DFT) studies and computational calculations were performed. Computed energies of the products in the reactions were calculated using theoretical data (Köse *et al*. 2020). Physical and theoretical formation energy calculations were performed to better explain the mechanisms of the products obtained.

2. Materials and Methods

The experimental procedures for all products have been reported in detail in our previous papers (Köse *et al.* 2017 and 2020). The reader is invited to access this information for additional data concerning this article.

2.1 General

All chemical solvents and reagents were used as received (Sigma-Aldrich). NMR spectra were recorded in $CHCl_3$-d_1 using a 400 MHz Bruker spectrometer for ^1H NMR and a 100 MHz Bruker spectrometer for ^{13}C NMR. Thin-layer chromatography (TLC) was visualized using UV light.

2.2 General procedure for the ether cleavage step with Ac_2O

Corresponding tricyclic imides (1.0 g) were dissolved in Ac_2O (5 mL) and 3-4 drops of H_2SO_4 was added at room temperature. The resulting solution was stirred at the times indicated in Figures 5a and 5b at rt. Aliquots were occasionally taken from the reaction medium to determine the consumption of tricyclic imide. Upon completion of diacetate formation, the mixture was concentrated under reduced pressure. The crude product was crystallized from dichloromethane/hexane. The crystals were obtained by filtration.

2.3 General procedure for the ether cleavage step with AcCl

To a stirring solution of corresponding tricyclic imides (1.0 g) in CH_2Cl_2 (10 mL) were added AcCl (4 mL) and 3-4 drops of H_2SO_4 at room temperature. The resulting solution was stirred at the times indicated in Figures 5a and 5b at rt. Aliquots were taken from the reaction medium to determine the

conversion from diacetate to chloroacetate. After the conversion of diacetate (indicated by ^{1}H NMR), the mixture was filtered and the filtrate was concentrated under reduced pressure. The residue was diluted with CH_2Cl_2 and crystallized with hexane. The crystals were filtered and washed with fresh hexane.

3. Results and Discussions

3.1. Overview

The aim in this study was to prove that the chlorinated monoacetate products (**5b**-**9b**) forming during the ether cleavage reaction with AcCl proceed through the diacetate products (**5a**-**9a**), which form firstly, and to demonstrate this transformation spectroscopically. In accordance with this purpose, Ac_2O only was firstly used for the ether cleavage of the starting compounds (**5**-**9**) and it was determined that *trans*-1,4-diacetates were the products. When these starting compounds were treated with AcCl, diacetates, which formed in the previous reaction, were determined first. For this, aliquots were taken from the reaction medium with AcCl at specific times and their NMR spectra were examined. A careful examination of the spectra showed that the diacetate product formed in the reaction medium firstly. As the reaction proceeded, the diacetate transformed into the chloroacetate gradually and then finally was completely consumed. This conversion, which was determined using NMR integration data, was observed with *N*-methyl-, *N*-benzyl- and *N*-acetoxyethyl-substituted norcantharimide derivatives. The other two derivatives (*N*-ethyl and *N*-phenyl) were excluded from this work since they have not been studied.

Reaction 1

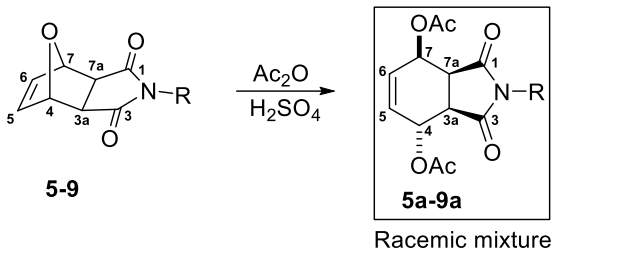

Mechanism 1

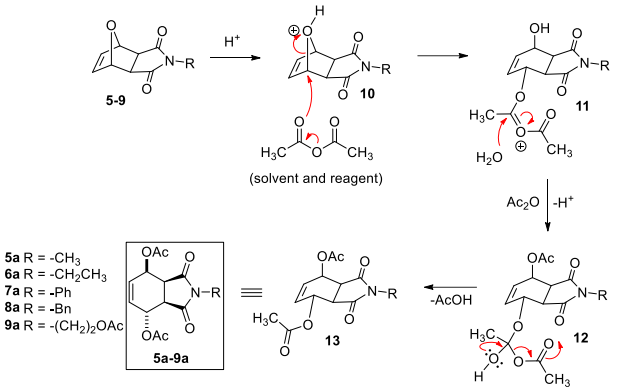

Reaction 2

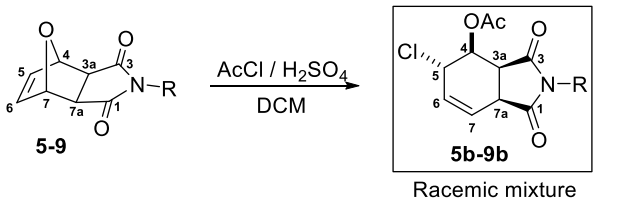

Mechanism 2

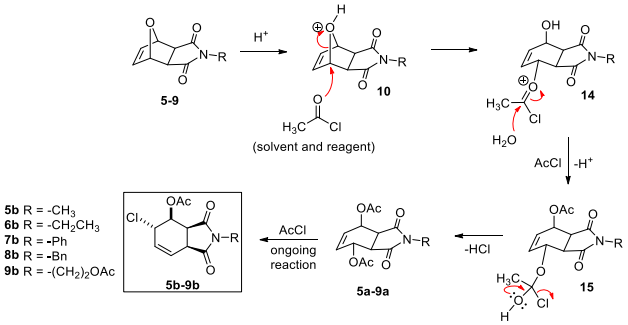

Figure 2. The reaction mechanisms of the formation of racemic *trans*-1,4-diacetates **5a**-**9a** and racemic *trans*-1,2-chloroacetates **5b**-**9b** because of stereospecific ether cleavage of *exo*-4,7-epoxyisoindoline-1,3-diones **5**-**9** by using Ac_2O and AcCl, respectively, in the presence of H_2SO_4.

Baran *et al*. conducted cleavage reactions with internal ethers in an acidic medium. In their research, instead of 1,2-chloroacetates, 1,4-chloroacetates were formed as the sole product. They performed an S_Ni reaction and *cis*-1,4-

chloroacetates were synthesized (Baran *et al*. 2003 and 2004). By application of their methodology, the etheric bonds in norcantharimide derivatives were subjected to cleavage reactions using Ac_2O or AcCl. The products and their formation mechanisms resulting from the ring-opening reactions with Ac_2O and AcCl appear to be as described in mechanisms 1 and 2 in Figure 2. Since the formation of the product in the cleavage reaction with AcCl took a long time, a detailed study was designed to establish how this product formed, unlike in the previous article (Köse *et al*. 2020). Surprisingly, it was found with the help of the ^1H NMR spectra that the *trans*-1,2-chloroacetate formed in this reaction according to the S_N2' mechanism progressed from the *trans*-1,4-diacetate that formed first as in the cleavage reaction with Ac_2O, as well.

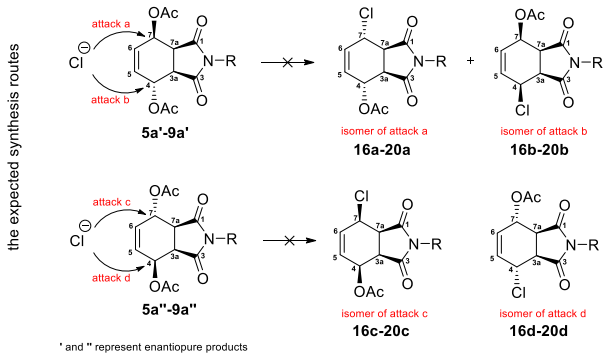

Figure 3. The structure of the expected stereoisomer products **16a-20a**, **16b-20b**, **16c-20c,** and **16d-20d** at the end of the reaction time in the reaction with AcCl.

First, when the NMR results were analysed, it was thought that the reaction mechanism proceeded as in Figure 3 because the NMR results and the expected products were in agreement. However, due to doubt, the structures were crystallized and X-ray analysis was performed (Köse *et al*. 2020). Here, it was seen that the diastereomeric products in Figure 4 were formed instead of the expected diastereomeric products in Figure 3.

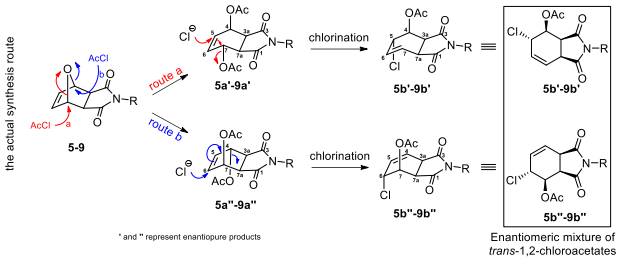

Figure 4. The structures and mechanistically synthetic routes of the enantiomeric final products **5b'-9b'** and **5b''-9b''** at the end of the reaction time in the reaction with AcCl.

Looking at the structures of the products of **5-9** it can be clearly seen that this tricyclic compound has an axis of symmetry and therefore bridgehead carbons and protons are identical and have the same steric area (Figure 4). Due to this feature, AcCl attacked both bridgehead carbons equally and the symmetry was broken. Following the formation of enantiomeric **5a'-9a'** and **5a''-9a''**, a chlorination reaction occurred (Figure 4). If the chloride had attacked the carbons where the acetates were attached according to the expected synthesis routes in Figure 3, the formation of the regioisomers in Figure 3 would have been required. However, the reaction did not progress that way. The chloride ion attacked the olefinic carbons according to the mechanism in Figure 4 and the products were formed as an enantiomeric mixture according to the S_N2' mechanism. The attack direction of the chloride was determined by X-ray analysis in our previous study. Based on the results of that analysis, we proved that the five membered ring and chlorine atom were *trans* in that article. Moreover, the steric hindrance is lower at the *endo*-directed attack of chloride. If chloride had attacked from the *exo* face of **5a'-9a'** and **5a''-9a''**, product **17** would have been formed (for **17** see table 1). There was some information lacking about the detailed mechanism of the formation and conversion from **5a'-9a'** and **5a''-9a''** of these enantiomers (**5b'-9b'** and **5b''-9b''**) in the earlier paper (Köse *et al*. 2020). In this paper, this mechanism was elucidated. The conversion times and quantitative ratios of the *trans*-1,2-chloroacetate products were determined by NMR spectroscopy. Additionally, the reason why the

expected products/isomers in Figure 3 did not occur was proved by DFT analysis.

3.2 Detailed Reaction Tracing

To further clarify the mechanism and conversion, aliquots were taken from the reaction medium at regular periods during the formation of the chloroacetate with AcCl and NMR analyses of these samples were performed. It was seen that the diacetate product formed in the reaction medium firstly. As the reaction continued, the heights of peaks belonging to the diacetate decreased and the heights of peaks belonging to the chloroacetate increased. Because of this conversion, the chloroacetate formed as a single product after consumption of the diacetate. It was deduced that the chloride performed a nucleophilic attack at C5 and C6 on **5a'**-**9a'** and **5a''**-**9a''** in the actual synthetic route instead of at C7 and C4 as in the expected synthetic route and therefore the chloroacetate formed following an S_N2' mechanism as an enantiomeric mixture (Figure 4). Here it is clearly explained when the chloroacetate began to form and how long completion of the conversion took.

In the reaction that used AcCl, the reaction mixture was initially colourless, then turned light green, and after 8-10 h turned dark green under the daylight. This coloration indicated that the reaction was progressing from the diacetate product to the chloroacetate product. The work was carried out with internal ethers **5**, **8**, and **9**.

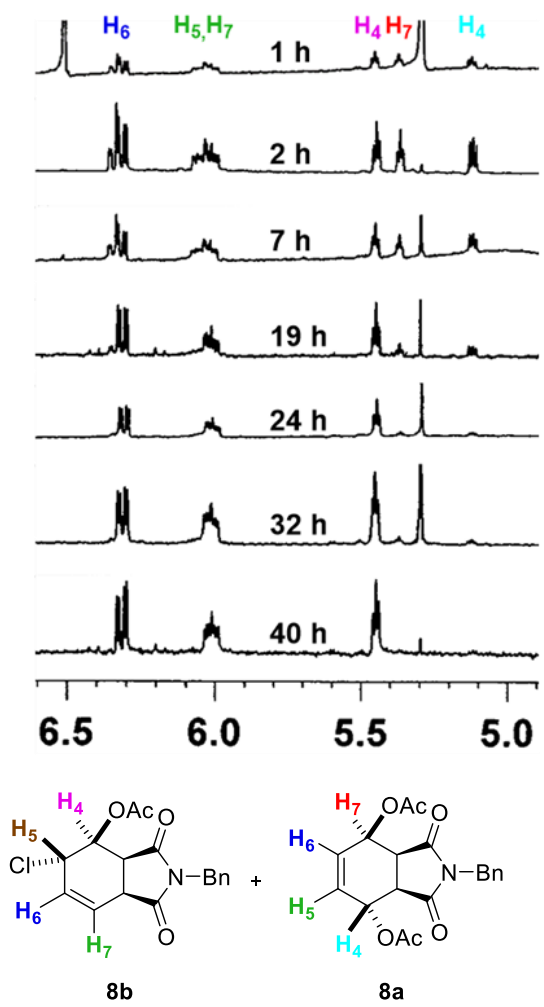

Figure 5a. This column shows ^{1}H NMR spectra taken from the reaction of **8** with AcCl at 1, 2, 7, 19, 24, 32 and 40 hours.

Figures 5a and 5b show the ^{1}H NMR spectra of **5a**, **5b** and **8a**, **8b,** respectively, at the specified reaction times. The ^{1}H NMR spectra seen in the Figure 5a and 5b were obtained from the reactions with AcCl of the two compounds (**5** and **8**) substituted with methyl and benzyl groups on the nitrogen under the same conditions. The spectra seen in the Figure 5a belong to compound **5** at reaction times 1, 7, 24, 32, 44, 67, and 90 hours in the presence of AcCl.

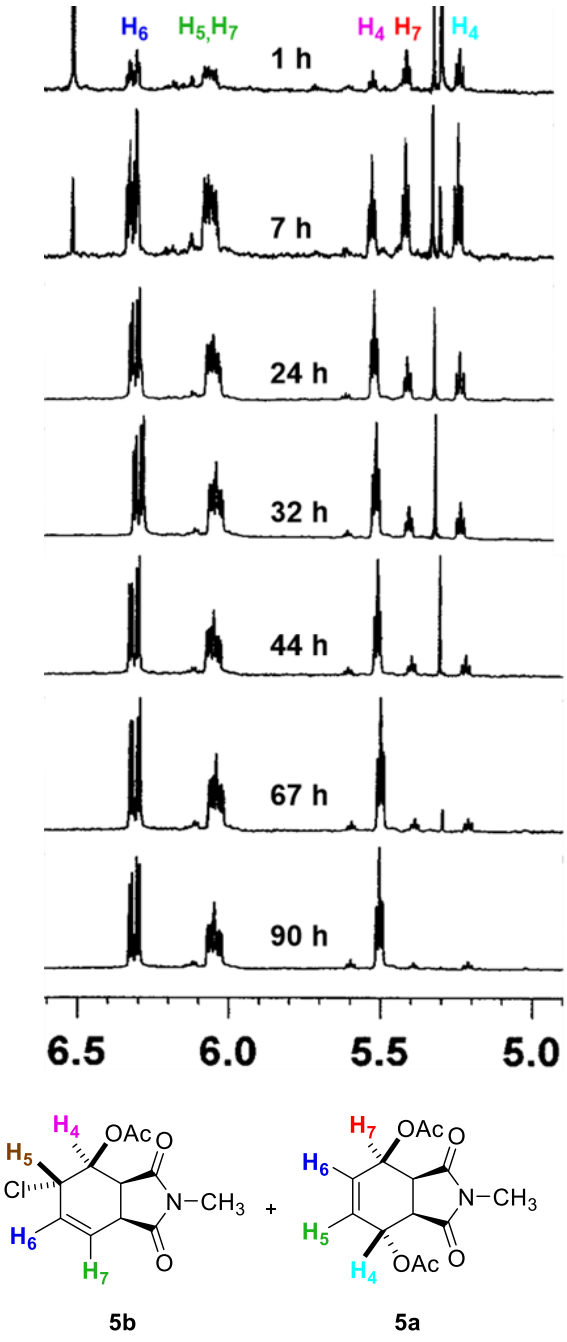

5b **5a**

Figure 5b. This column shows ^{1}H NMR spectra taken from the reaction of **5** with AcCl at 1, 7, 24, 32, 44, 67, and 90 hours.

Those seen in the figure 5a belong to compound **8** at reaction times 1, 2, 7, 19, 24, 32, and 40 hours with AcCl. Before analysing these spectra, it was considered useful to determine which peaks belonged to which protons.

3.3 Analyses of NMR spectra

The signal at 6.3 ppm seen in both columns as a doublet of doublet (*dd*) belonged to the olefinic **H6** protons for both *trans*-1,2-chloroacetates (**5b** and **8b**) and *trans*-1,4-diacetates (**5a** and **8a**). The other olefinic protons **H5** in **5a** and **8a** and **H7** in **5b** and **8b** resonated at 6.05 ppm as a multiplet (*m*) and the signals overlapped. In the spectra in the left column, the signal at 5.5 ppm belonged to **H4** for **5b**. In the spectra in the right column, the signal of this proton was seen at 5.45 ppm for **8b** (Figures 5a and 5b). This **H4** proton belonged to the *trans*-1,2-chloroacetates (**5b** and **8b**) and was also geminal to the acetate group. The signals seen at 5.4 ppm and 5.2 ppm in the left spectra belonged to **H7** and **H4** protons for **5a** and **8a**, respectively. These signals resonated at 5.37 ppm and 5.12 ppm in the right spectra. It was determined that *trans*-1,4-diacetate and *trans*-1,2-chloroacetate in 4:1 stoichiometry for an hour in the reaction of **9a** and **9b**. As the reaction continued, it was seen that the heights of the signals belonging to *trans*-1,4-diacetate decreased. Simultaneously, the heights of the signals belonging to *trans*-1,2-chloroacetate increased. According to this result, an intermolecular transformation from *trans*-1,4-diacetate to *trans*-1,2-chloroacetate was occurring and it was detected that *trans*-1,2-chloroacetate was synthesized from *trans*-1,4-diacetate. Moreover, based on the integrations in the NMR spectra, the ratio of *trans*-1,4-diacetate to *trans*-1,2-chloroacetate in the reaction mixture was observed to decrease proportionally with the reaction time. Integration bars are not specified in the spectra shown in Figures 5a and 5b. The reader is invited to refer to the spectra with integration provided in the supporting information section of the online version of this article.

As mentioned in detail in the mechanism part, the location of the double bond in **5a**-**9a** shifted with the intermolecular transformation via the S_N2' mechanism. In spite of this migration, no substantial chemical shift was observed in the olefinic signals in the NMR spectra during the reaction. The signal at 4.5 ppm belonging to the **H5** proton in **5b** and **8b**, which was in the geminal position with the chlorine atom and is shown in brown, is not specified in Figures 5a and 5b. Nevertheless, it was determined that the height of this signal increased

proportionally with the signal of **H4** at the same time.

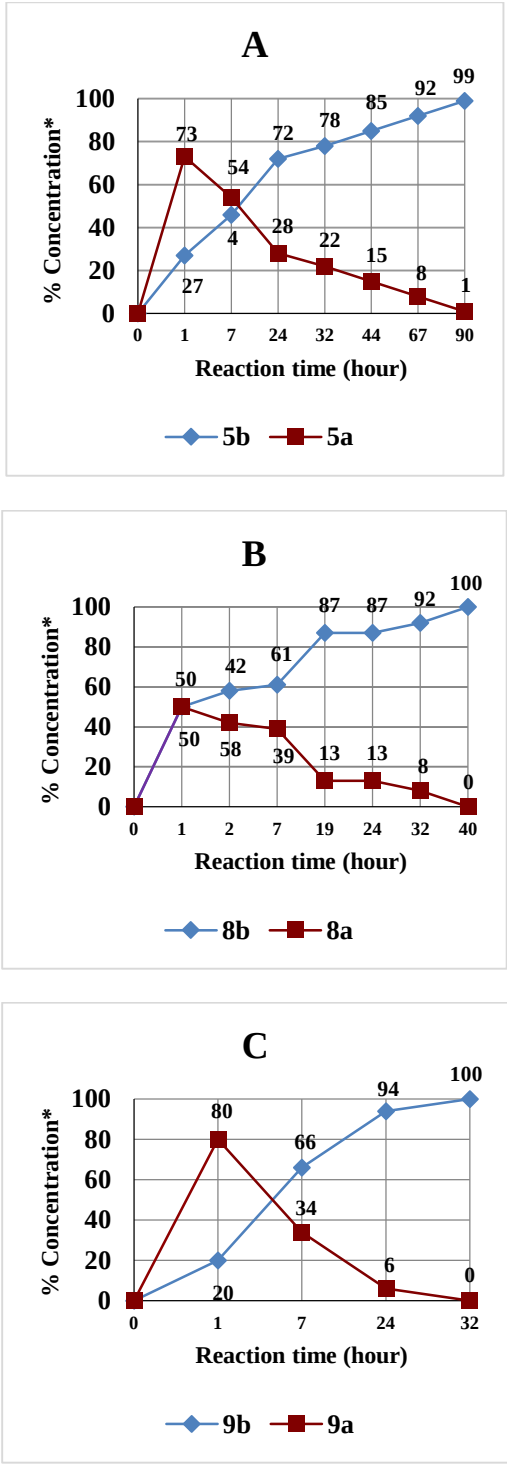

Figure 6. Concentration (%) / reaction time (hour) graphs of *trans*-1,4-diacetates and *trans*-1,2-chloroacetates obtained from **5**, **8,** and **9.** Graph **A** shows the concentration of **5b** and **5a**, graph **B** shows the concentration of **8b** and **8a**, and graph **C** shows the concentration of **9b** and **9a** relative to each other over time.

3.4 Graphic depiction of the products

It was demonstrated by ^{1}H NMR spectroscopy that the *trans*-1,2-chloroacetate product was synthesized in the ether cleavage reaction with AcCl formed from a *trans*-1,4-diacetate intermediate, which formed firstly for all reactions. The graphs display the concentration (%) of the conversion of *trans*-1,4-diacetate to trans-1,2-chloroacetate over time (Figure 6). These graphs were designed using the integration data in the ^{1}H NMR spectra of the synthesized products because of the cleavage reactions of compounds **5**, **8**, and **9** with AcCl. A careful examination of the graphs shows that the concentrations of *trans*-1,4-diacetate and *trans*-1,2-chlorocetate were 1:3 for **5b** and **5a,** respectively, at the end of one hour of reaction time. This ratio was 1:1 between **8a** and **8b** and between **9a** and **9b**. As indicated in graph A, the concentration of *trans*-1,4-diacetate product **5a** was 73% in the first hour and after 26 hours the concentration decreased to 22%. In the other graphs, the concentration of *trans*-1,4-diacetate was 13% for **8a** and 6% for **9a** at this time. This result indicates that it could be said that the synthesis of the *trans*-1,2-chloroacetate **5b** was slower than that of other *trans*-1,2-chloroacetates **8b** and **9b**. The reason was thought to be the intramolecular Van der Waals interactions for **8**. The extended synthesis time of *trans*-1,2-chloroacetate **8a** from **8** showed that this interaction was quite strong compared to that of **8** and **9**. The intermolecular conversion from *trans*-1,4-diacetate to *trans*-1,2-chloroacetate required 4 days for the reaction of **5**, 40 h for the reaction of **8,** and 32 h for the reaction of **9**. As outlined in graphic C in Figure 6, the synthesis of **9b** took less time compared to the syntheses of **5b** and **8b**, even though **9b** was the most sterically bulky and substituted heteroatoms at nitrogen. Nevertheless, the formation time of **9b** showed that this steric effect did not hinder the reaction. Additionally, when the amount of acid was increased, the synthesis time of *trans*-1,2-chloroacetate decreased but the aromatized product began to form.

3.5 Computational Part

To further explain the formation of **5b** and better understand the behaviour of **5a**, DFT with the B3LYP functional (Lee *et al*. 1988) was used via the program Gaussian 09 (Frisch *et al*. 2009). All energies reported in the results and discussion were calculated at the B3LYP/6-311G(d,p) level and include unscaled zero-point vibrational energies.

Computational studies showed that the energy of *trans*-1,2-chloroacetate resulting from the transformation was lower than that of *trans*-1,4-diacetate, which first occurred in the reaction. The *trans*-1,2-chloroacetate product formed because of the reaction with AcCl, and the formation energies of the isomers of this structure are given in Table 1 in kcal/mol. This table shows that in the ongoing reaction with AcCl the attack aspects of the chloride ion that formed in the same reaction medium was supported exactly. Moreover, the stereochemistry and absolute configuration of these chlorinated products, formed as an enantiomeric mixture following the S_N2' mechanism, were verified by computational calculations. These computational results clearly revealed that compound **5b** was preferable and the difference in energies between them proved this theoretically

Table 1. Formation energies of all possible products (in hartree/particle), including Zero-Point corrections and relative energy differences (kcal/mol) for **5b**, **17**, **16a**, and **18** respectively.

Compounds	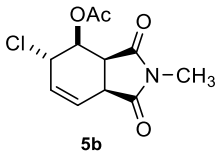 **5b**	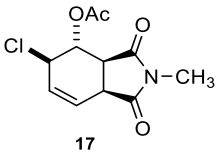 **17**	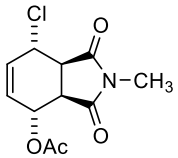 **16a**	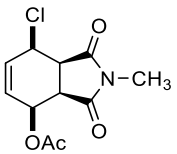 **18**
Computed structures	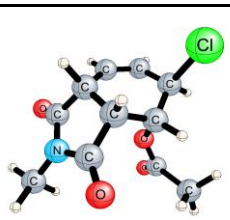	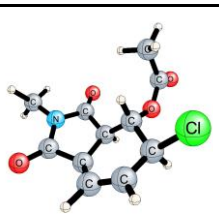	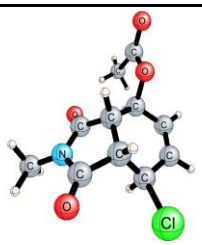	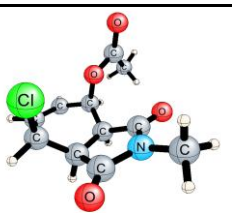
Energy values	-1242.28027650	-1242.27682650	-1242.27042600	-1242.26581230
Formation energy differences kcal/mol (between **5b** and others)	0.0	2.2	6.2	9.1

4. Conclusion

In this study, the ether bonds of **5**, **8**, and **9** were subjected to cleavage reactions to give **5a**, **8a**, **9a**, **5b**, **8b**, and **9b** in the presence of Ac_2O or AcCl and H_2SO_4 as catalyst. First, the ether cleavage reaction was performed using Ac_2O and *trans*-1,4-diacetates (**5a**, **8a**, and **9a**) were synthesized. The mechanism of these reactions was explained in detail. Second, the ether cleavage reactions of **5**, **8**, and **9** were performed using AcCl and it was determined that *trans*-1,2-chloroacetates **5b**, **8b**, and **9b** were the products instead of the expected *cis*-1,4-chloroacetates **16a-d** and **20a-d**. Studies such as ^1H NMR and theoretical calculations were conducted to determine the mechanism. The results of these studies were discussed in detail. First, the mechanism of the reaction of **5**, **8**, and **9** with AcCl was explained by identifying and monitoring the

reaction intermediates and products with ^{1}H NMR spectroscopy. It was determined that **5b**, **8b**, and **9b** formed through the *trans*-1,4-diacetate intermediates **5a**, **8a**, and **9a** in the reaction medium over time. The stoichiometric proportions of the products (*trans*-1,4-diacetate and *trans*-1,2-chloroacetate) formed because of the ether cleavage reaction with AcCl of **5**, **8**, and **9** were measured via integrals of ^{1}H NMR spectra of aliquots taken from the reaction at certain time points. Based on these findings, *trans*-1,2-chloroacetate began to occur from the corresponding *trans*-1,4-diacetate over time via an S_N2' mechanism. These results were reinforced by theoretical calculations. The formation energies of **5b** and its isomers were calculated and it was determined that the formation of **5b** was preferential computationally.

Caution: During the method described here, when an excess amount of AcCl is removed under reduced pressure, suffocating AcCl and HCl gases are released from the vacuum pump if not adequately trapped or ventilated in a fume hood. Appropriate precautions should be taken during this procedure.

Supporting Information: Aliquot NMR spectra, characterized spectra of the compounds, and computations with the B3LYP/6-311G(d,p) statistics for the optimized structures are provided in the Supporting Information

5. References

Baran, A., Kazaz, C., Seçen, H., Sütbeyaz, Y. (2003). Synthesis of haloconduritols from an endo-cycloadduct of furan and vinylene carbonate. *Tetrahedron.* 59, **20**, 3643-3648. https://doi.org/10.1016/S0040-4020(03)00510-6

Baran, A., Kazaz, C., Seçen, H. (2004). Stereoselective ring-opening reactions with AcBr and AcCl. A new method for preparation of some haloconduritols. *Tetrahedron.* 60, **4**, 861-866. https://doi.org/10.1016/j.tet.2003.11.054

Frisch, M.J., Trucks, G.W., Schlegel, H.B., Scuseria, G.E., Robb, M.A., Cheeseman, J.R., Scalmani, G., Barone, V., Mennucci, B., Petersson, G.A., Nakatsuji, H., Caricato, M., Li, X., Hratchian, H. P., Izmaylov, A.F., Bloino, J., Zheng, G., Sonnenberg, J.L., Hada, M., Ehara, M., Toyota, K., Fukuda, R., Hasegawa, J., Ishida, M., Nakajima, T., Honda, Y., Kitao, O., Nakai, H., Vreven, T., Montgomery, J.A.Jr., Peralta, J. E., Ogliaro, F., Bearpark, M., Heyd, J.J., Brothers, E., Kudin, K.N., Staroverov, V.N., Kobayashi, R., Normand, J., Raghavachari, K., Rendell, A., Burant, J.C., Iyengar, S.S., Tomasi, J., Cossi, M., Rega, N., Millam, J.M., Klene, M., Knox, J.E., Cross, J.B., Bakken, V., Adamo, C., Jaramillo, J., Gomperts, R., Stratmann, R.E., Yazyev, O., Austin, A.J., Cammi, R., Pomelli, C., Ochterski, J. W., Martin, R.L., Morokuma, K., Zakrzewski, V. G., Voth, G.A., Salvador, P., Dannenberg, J.J., Dapprich, S., Daniels, A.D., Farkas, Ö., Foresman, J.B., Ortiz, J.V., Cioslowski, J., Fox, D.J. (2009), Gaussian 09, Gaussian, Inc.: Wallingford, CT.

Köse, A., Bal, Y., Kishalı, N.H., Şanlı-Mohamed, G., Kara, Y. (2017). Synthesis and anticancer activity evaluation of new isoindole analogues. *Medicinal Chemistry Research*. 26, **4**, 779-786. https://doi.org/10.1007/s00044-017-1793-1

Köse, A., Kaya, M., Kishalı, N.H., Akdemir, A., Şahin, E., Kara, Y., Şanlı-Mohamed, G. (2020). Synthesis and biological evaluation of New Chloro/Acetoxy Substituted Isoindole Analogues as new tyrosine kinase inhibitors. *Bioorganic Chemistry*. **94**, 103421. https://doi.org/10.1016/j.bioorg.2019.103421

Lee, C., Yang, W. and Parr, R.G. Development of the Colic-Salvetti correlation-energy formula into a functional of the electron density. (1988). *Physical Review B.* 37, **2**, 785-789. https://doi.org/10.1103/PhysRevB.37.785

Lin, P.Y., Shi, S.J., Hsu, F.L., Chen, C.F. (1998). New Cantharidinimides from Cantharidin and 2-Arylethylamines: Efficient Synthesis under High Pressure.. *Journal of the Chinese Chemical*

Society. 45, **2**, 323-326. https://doi.org/10.1002/jccs.199800052

Nickolls, L.C., and Teare, D. (1954). Poisoning By Cantharidin. *British Medical Journal*. 1954; 2, **4901**, 1384-1386. https://www.jstor.org/stable/20361797

Tagwireyi, D., Ball, D.E., Loga, P.J., Moyo, S. (2000). Cantharidin poisoning due to "Blister beetle" ingestion. *Toxicon*. 38, **12**, 1865-1869. https://doi.org/10.1016/s0041-0101(00)00093-3

Tan, A., Koc, B., Sahin, E., Kishali, N.H., Kara, Y. (2011). Synthesis of New Cantharimide Analogues Derived from 3-Sulfolene. *Synthesis*. **7**, 1079- https://doi.org/10.1055/s-0030-1258466

Tan, A., Bozkurt, E., Kishali, N., Kara, Y. (2014). A New and Convenient Synthesis of Amino-phthalimide (1*H*-Isoindole1,3(2*H*)-dione) Derivatives and Their Photoluminescent Properties. *Helvetica Chimica Acta*. 97, **8**, 1107-1114. https://doi.org/10.1002/hlca.201300394

Wang, G.S. (1989). Medical Uses of Mylabris in Ancient China and Recent Studies. *Journal of Ethnopharmacology*. 26, **2**, 147-162. https://doi.org/10.1016/0378-8741(89)90062-7